

DEPARTMENT OF ELECTRICAL AND COMPUTER ENGINEERING  
COLLEGE OF SCIENCES  
OLD DOMINION UNIVERSITY  
NORFOLK, VIRGINIA 23529

**GUIDANCE AND CONTROL STRATEGIES  
FOR AEROSPACE VEHICLES**

By

Desineni S. Naidu, Research Associate

Joseph L. Hibey, Principal Investigator

Progress Report

For the period July 1, 1988 through December 31,  
1988

Prepared for the  
National Aeronautics and Space Administration  
Langley Research Center  
Hampton, Virginia 23665-5225

Under

Research Grant NAG-1-736

Dr. Douglas B. Price, Technical Monitor  
GCD-Spacecraft Control Branch

(NASA-CR-182339) GUIDANCE AND CONTROL  
STRATEGIES FOR AEROSPACE VEHICLES Progress  
Report, 1 Jul. - 31 Dec. 1988 (Old Dominion  
Univ.) 41 p CSCI 01C

N89-15927

Unclas  
G3/08 0185464

January 1989

DEPARTMENT OF ELECTRICAL AND COMPUTER ENGINEERING  
COLLEGE OF SCIENCES  
OLD DOMINION UNIVERSITY  
NORFOLK, VIRGINIA 23529

**GUIDANCE AND CONTROL STRATEGIES  
FOR AEROSPACE VEHICLES**

By

Desineni S. Naidu, Research Associate

Joseph L. Hibey, Principal Investigator

Progress Report  
For the period July 1, 1988 through December 31,  
1988

Prepared for the  
National Aeronautics and Space Administration  
Langley Research Center  
Hampton, Virginia 23665-5225

Under  
Research Grant NAG-1-736  
Dr. Douglas B. Price, Technical Monitor  
GCD-Spacecraft Control Branch

Submitted by the  
Old Dominion University Research Foundation  
P. O. Box 6369  
Norfolk, Virginia 23508

January 1989

**GUIDANCE AND CONTROL STRATEGIES  
FOR AEROSPACE VEHICLES**

By

Desineni S. Naidu<sup>1</sup> and Joseph L. Hibey<sup>2</sup>

**SUMMARY**

Enclosed is a List of Publications/Reports, a conference paper and a report on the above titled project for the period July 1, 1988 through December 31, 1988.

---

<sup>1</sup>Research Associate, Department of Electrical and Computer Engineering, Old Dominion University, Norfolk, Virginia 23529.

<sup>2</sup>Associate Professor, Department of Electrical and Computer Engineering, Old Dominion University, Norfolk, Virginia 23529.

### List of Publications/Reports

(i) D. S. Naidu and D. B. Price, "Singular Perturbation and Time Scale Approaches in Discrete Control Systems", Journal of Guidance, Control and Dynamics, Vol., 11, no. 5, pp. 592-594, Nov.-Dec., 1988.

(ii) D. S. Naidu and D. B. Price, "Singular Perturbations and Time Scales in the Design of Digital Flight Control Systems", NASA Technical Paper 2844, Langley Research Center, Hampton, December 1988

\*(iii) D. S. Naidu, J. L. Hibey, and C. Charalambous, "Optimal Control of Aeroassisted, Coplanar, Orbital Transfer Vehicles", 26 IEEE Conference on Decision and Control, Austin, Texas, December 7-9, 1988.

(iv) D. S. Naidu and D. B. Price, "On the Method of Matched Asymptotic Expansions", accepted for publication in Journal of Guidance, Control and Dynamics, 1989 (in press).

(v) D. S. Naidu, "There-Dimensional Atmospheric Entry Problem using Method of Matched Asymptotic Expansions", accepted for publication in IEEE Transactions on Aerospace and Electronic Systems, 1989.

\*(vi) D. S. Naidu, "Fuel-Optimal Trajectories of Aeroassisted Orbital Transfer Vehicles", Report, ODU Research Foundation, Norfolk, VA, January, 1989.

(vii) D. S. Naidu, and D. B. Price, "Fuel-Optimal Trajectories of Aeroassisted Orbital Transfer with Plane Change," Submitted for AIAA Guidance, Navigation, and Control Conference, Boston, MA, August 14-16, 1989.

\* copies enclosed

\*\*\*\*\*

**FUEL-OPTIMAL TRAJECTORIES FOR AEROASSISTED  
COPLANAR ORBITAL TRANSFER PROBLEM**

Dr. D. S. Naidu<sup>\*</sup>, Dr. J. L. Hibey<sup>@</sup>, and C. Charalambous<sup>#</sup>  
Department of Electrical and Computer Engineering  
Old Dominion University  
Norfolk, VA, 23529

THE 27th IEEE CONFERENCE ON DECISION AND CONTROL  
Austin, Texas, December 7-9, 1988

<sup>\*</sup> Associate Professor (Research), <sup>@</sup> Associate Professor  
<sup>#</sup> Graduate Student

# FUEL-OPTIMAL TRAJECTORIES FOR AEROASSISTED COPLANAR ORBITAL TRANSFER PROBLEM

D. S. Naidu, J. L. Hibey, and C. Charalambous

Department of Electrical and Computer Engineering  
Old Dominion University  
Norfolk, VA, 23529

ORIGINAL PAGE IS  
OF POOR QUALITY

## ABSTRACT

The optimal control problem arising in coplanar, orbital transfer employing aeroassist technology is addressed. The maneuver involves the transfer from high Earth orbit to low Earth orbit with minimum fuel consumption. Simulations are carried out for obtaining a corridor of entry conditions which are suitable for flying the spacecraft through the atmosphere. A highlight of the paper is the application of an efficient multiple shooting method for taming the notorious non-linear, two-point, boundary value problem resulting from the optimization procedure.

## NOMENCLATURE

$A = Sp_a/2m$ ;  $A_1 = C_{DO} Sp_a H_a/2m$ ;  $A_2 = C_{LR} Sp_a H_a/2m$   
 $a_c = R_c/R_a$ ;  $a_d = R_d/R_a$ ;  $b = R_a/H_a$ ;  $C_D = C_{DO} + KC_L^2$   
 $C_{DO}$ : zero-lift drag coefficient  
 $C_L$ : lift coefficient;  $C_{LR} = \sqrt{C_{DO}/K}$ ;  $c = C_L/C_{LR}$   
 $E_a = (L/D)_{max}$ ;  $g$ : gravitational acceleration  
 $H$ : altitude;  $h = H/H_a$ ;  $J$ : performance index  
 $K$ : induced drag factor;  $m$ : vehicle mass  
 $R$ : distance from Earth center  
 $R_a$ : radius of the atmosphere;  $R_E$ : radius of Earth  
 $S$ : aerodynamic reference area  
 $t$ : time;  $v = V/\sqrt{\mu/R_a}$ ;  $\beta$ : inverse scale height  
 $\gamma$ : flight path angle;  $\delta = \exp(-h\beta H_a)$   
 $\lambda$ : costate variable;  $\mu$ : gravitational constant  
 $\rho$ : density;  $\tau = t/\sqrt{R_a^3/\mu}$   
 $\Delta v$ : characteristic velocity

## Subscripts

$c$ : circularization or reorbit;  $d$ : deorbit  
 $e$ : entry to atmosphere;  $f$ : exit from atmosphere

## I. INTRODUCTION

In this paper, we address the fuel-optimal control problem arising in coplanar orbital transfer employing aeroassist technology [1-3]. The maneuver involves a transfer from high Earth orbit (HEO) to low Earth orbit (LEO) with minimum fuel consumption. A suitable performance index is the sum of the characteristic velocities for deorbit and reorbit (or circularization) [4]. Use of Pontryagin minimum principle leads to a two-point boundary value problem (TPBVP) in state and costate variables. This problem is solved by using an efficient multiple shooting method [5] in preference to the sequential gradient-restoration algorithm [4]. In addition, simulations are carried out for obtaining a spectrum of entry conditions which are suitable for flying the spacecraft through the atmosphere.

## II. AEROASSISTED COPLANAR TRANSFER

In an aeroassisted, coplanar transfer, the vehicle is transferred from HEO at  $R_a$  to LEO at  $R_c$ , by flying deep into the atmosphere to achieve the necessary velocity reduction (Figure 1). We start with a tangential propulsive burn, having a characteristic velocity  $\Delta v_d$

for deorbiting from HEO and entering into an elliptical transfer orbit. At point E the spacecraft enters the atmosphere with flight path angle  $\gamma_e$  and undergoes reduction in velocity due to atmospheric drag. At point F, the spacecraft leaves the atmosphere with flight path angle  $\gamma_f$ . Once again, the transfer orbit is elliptical with the corresponding apogee at  $R_c$ . Finally, the maneuver ends with a circularizing or reorbit burn having a characteristic velocity  $\Delta v_c$  to make the vehicle enter into the low Earth orbit. Thus, the maneuver consists of two impulses  $\Delta v_d$  for deorbit, and  $\Delta v_c$  for circularization and is assumed to take place right at the perigee itself.

## Equations of Motion

Consider a vehicle with constant point mass, moving about a nonrotating spherical planet. The atmosphere surrounding the planet is assumed to be at rest, and the central gravitational field obeys the usual inverse square law. The equations of motion are given by

$$\frac{dH}{dt} = V \sin \gamma \quad (1a)$$

$$\frac{dV}{dt} = -AC_D V^2 \exp(-H\beta) - (\mu/R^2) \sin \gamma \quad (1b)$$

$$\frac{d\gamma}{dt} = AC_L V \exp(-H\beta) + [V/R - \mu/(R^2 V)] \cos \gamma \quad (1c)$$

Using normalized values,

$$\frac{dh}{d\tau} = b v \sin \gamma \quad (2a)$$

$$\frac{dv}{d\tau} = -A_1 b(1+c^2)\delta v^2 - \frac{b^2 \sin \gamma}{(b-1+h)^2} \quad (2b)$$

$$\frac{d\gamma}{d\tau} = A_2 b c \delta v + \frac{b v \cos \gamma}{(b-1+h)} - \frac{b^2 \cos \gamma}{(b-1+h)^2 v} \quad (2c)$$

## Optimal Control

For minimum fuel consumption, the performance index is given by

$$J = \Delta v = \Delta v_d + \Delta v_c \quad (3)$$

where,

$$\Delta v_d = \sqrt{1/a_d} - (v_e/a_d) \cos(-\gamma_e) \quad (4a)$$

$$\Delta v_c = \sqrt{1/a_c} - (v_f/a_c) \cos(\gamma_f) \quad (4b)$$

We are interested in finding the minimization of the fuel with respect to the control  $C_L$ . Using Pontryagin's principle [4], the unconstrained optimal control is obtained as

$$c = E_a \lambda_\gamma / v \lambda_v \quad (5)$$

Realistically, the control  $C_L$  is bounded by the aerodynamic characteristics of the vehicle. The initial and final boundary conditions are given as  $h(\tau=0) = 1.0$ ;  $h(\tau=\tau_f) = 1.0$ . and

$$(2-v_e^2)a_d^2 - 2a_d + v_e^2 \cos^2 \gamma_e = 0 \quad (6a)$$

$$(2-v_f^2)a_c^2 - 2a_c + v_f^2 \cos^2 \gamma_f = 0 \quad (6b)$$

The remaining boundary conditions are obtained from the transversality conditions on the costates. Thus, the optimization procedure, requiring the solution of state and costate equations along with the boundary conditions leads us to the formation of a TPBVP, which is solved by using a multiple shooting method [5].

### III. NUMERICAL DATA AND RESULTS

A typical set of numerical values used for simulation purposes is given below [3].  $C_{D0} = 0.21$ ;  $K = 1.67$ ;

$m/S = 300 \text{ kg/m}^2$ ;  $\rho_e = 1.225 \text{ kg/m}^3$ ;  $\mu = 3.986 \times 10^{14} \text{ m}^3/\text{sec}^2$ ;  $\beta = 1/6900 \text{ m}^{-1}$ ;  $R_E = 6378 \text{ km}$ ;  $H_a = 120 \text{ km}$ ;  $R_d = 12996 \text{ km}$ ;  $R_c = 6558 \text{ km}$ . Figure 2(a) shows the time history of altitude. The spacecraft enters and exits the atmosphere at an altitude of 120 km. The minimum altitude reached is 55.58 km. The velocity versus time is shown in Figure 2(b). The vehicle enters the atmosphere with a velocity of 9029 m/sec and leaves the atmosphere with a speed of 7795 m/sec, thus giving a velocity reduction of 1234 m/sec. The profile of flight path angle with time is shown in Figure 2(c). The spacecraft enters the atmosphere with an inclination of -5.665 degrees and exits with +0.927 degrees. The control history is shown in Figure 2(d). The vehicle enters the atmosphere with maximum lift capability and switches to the minimum lift coefficient and then gradually increases during the remaining flight.

The minimum-fuel transfer requires a deorbit (impulse) characteristic velocity  $\Delta V_d$  of 1034.29 m/sec and a reorbit characteristic velocity  $\Delta V_c$  of 73.25 m/sec, with a total characteristic velocity of 1107.54 m/sec. Let us compare this aeroassisted transfer with the Hohmann transfer, which is maneuvered entirely in outer space, and has a total characteristic velocity of 2194.64 m/sec. This shows that the saving due to coplanar, aeroassisted transfer over Hohmann transfer is 49.54 percent. In the case of idealized transfer which follows a grazing trajectory along the atmospheric boundary, the total characteristic velocity is 1034.18 m/sec. The optimal transfer requires only 6.63 percent more fuel than that of the idealized transfer. The heating rate shows a peak value of 129.2 W/cm<sup>2</sup>, and the total integrated heating load is found to be 15.536 KW-sec/cm<sup>2</sup>. The peak dynamic pressure is 26.73 kN/sq.m and the density attains a maximum value of  $0.3902 \times 10^{-3} \text{ kg/m}^3$ .

#### Entry Corridor

A given vehicle cannot fly an acceptable atmospheric flight for arbitrary initial conditions at the entry point. If the flight path angle  $\gamma_e$  is too steep, the vehicle will later suffer excessive aerodynamic and aerothermodynamic loadings even if the maximum lift is directed upward. This also may lead to "crash" condition. Or if the entry flight path angle is too shallow, the vehicle will exit the atmosphere again with an orbital velocity even if the maximum lift is directed downward. This leads to "escape" or uncontrolled skip-out condition. These boundaries of entry flight path angle are often taken to define the

corridor of acceptable entry conditions.

The entry corridor is the entry interface undershoot and overshoot and is usually specified by the entry flight path angle  $\gamma_e$ , as dictated by the entry dynamics. In the present case of fuel-optimal, coplanar, orbital transfer, four simulations are carried out as shown below.

No	$\gamma_e$ deg	$V_e$ m/sec	$C_L$	flight time seconds
1	-7.240	9020	0.5381	510
2	-6.412	9025	0.5786	600
3	-5.665	9029	0.6299	540
4	-5.485	9030	0.6502	600

Figure 3 shows the successive approximations of the altitude  $H$ , during the course of 0, 5, and 14 iterations in using the multiple shooting method [5]. For the sake of clarity only 4 out of 20 intervals are shown. The initial guessed value for the altitude is 120 km at every interval. It can be seen how the initially large jumps at the subdivision points of the multiple shooting method are "flattened out" with the increase of iterations.

The strategy for the atmospheric portion of the minimum-fuel transfer is to fly at the maximum L/D initially in order to recover from the downward plunge, and then to fly at a negative L/D to level off the flight such that the vehicle skips out of the atmosphere with a flight path angle near zero degrees.

#### ACKNOWLEDGEMENTS

This research work was supported by grant NAG1-736 from NASA Langley Research Center, Hampton, under the technical monitorship of Dr Douglas B. Price, Assistant Head, Spacecraft Control Branch.

#### References

1. Walberg, G. D., "A survey of aeroassisted orbital transfer", J. Spacecraft, 22, pp.3-18, Jan.-Feb., 1985.
2. Mease, K. D., and Vinh, N. X., "Minimum-fuel aeroassisted coplanar orbit transfer using lift modulation", J. Guidance, Control, and Dynamics, Vol., 8, pp.134-141, Jan.-Feb., 1985.
3. Miele, A., Basapur, V. K., and Lee, W. Y., "Optimal trajectories for aeroassisted coplanar orbit transfer", J. Opt. Theory & Appl., 52, pp.1-24, Jan., 1987.
4. Marec, J. P., Optimal Space Trajectories, Elsevier Scientific Publishing Company, Amsterdam, 1979.
5. Stoer, J., and Bulirsch, R., Introduction to Numerical Analysis, Springer-Verlag, New York, 1980.

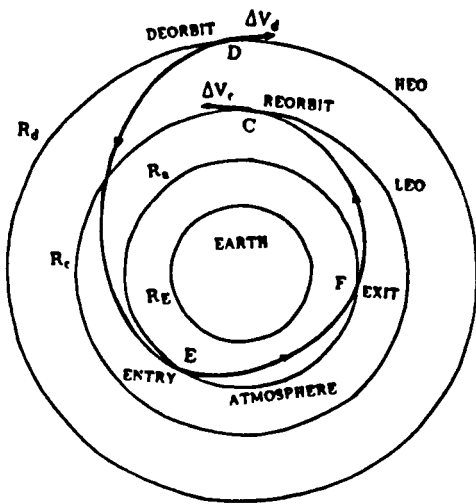


Figure 1 Aeroassisted coplanar orbital transfer

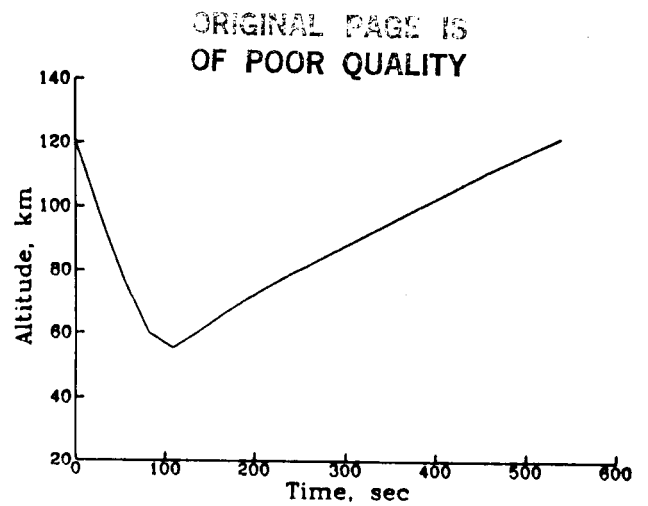


Figure 2(a) Time history of altitude

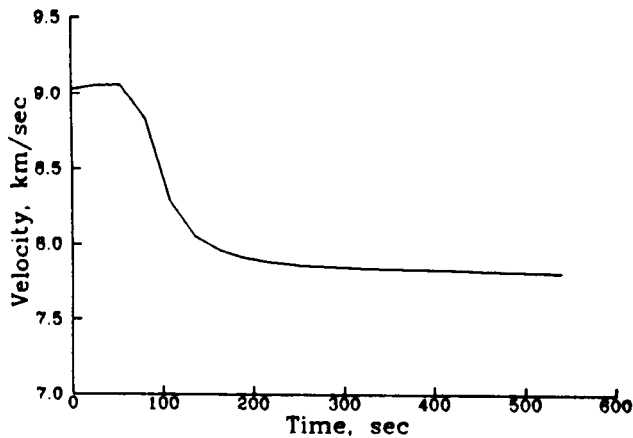


Figure 2(b) Time history of velocity

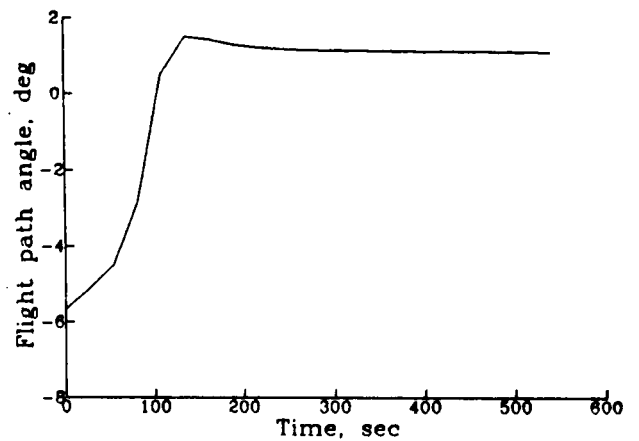


Figure 2(c) Time history of flight path angle

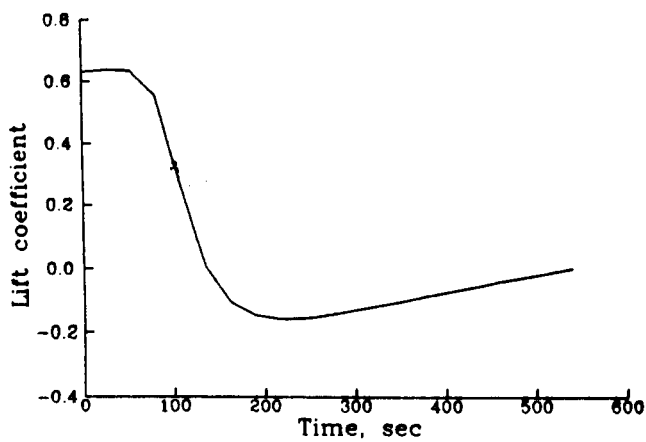


Figure 2(d) Time history of lift coefficient

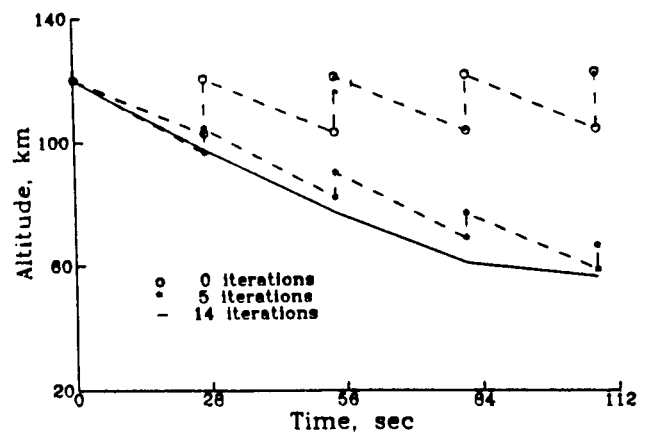


Figure 3 Successive approximations for altitude



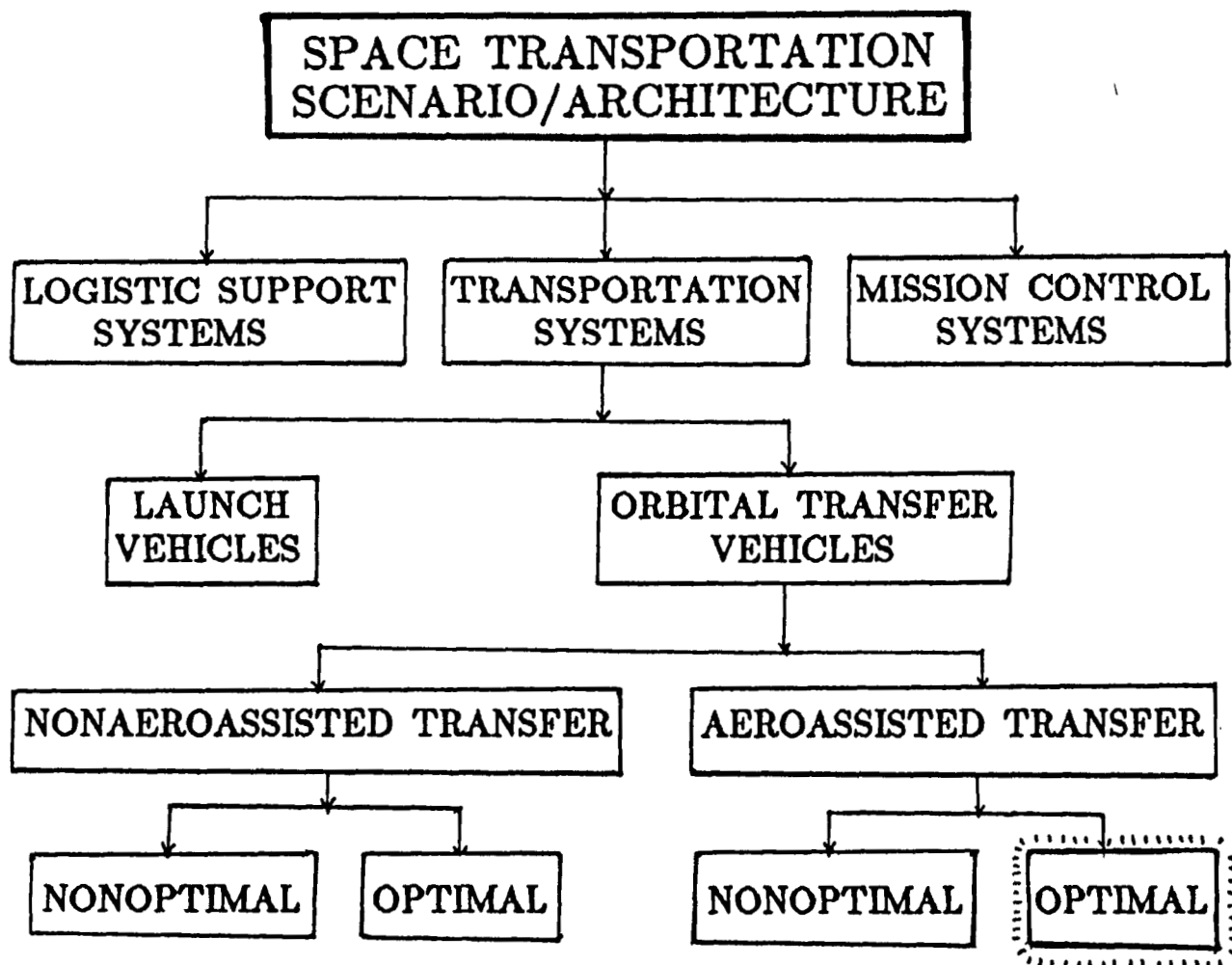
**FUEL—OPTIMAL TRAJECTORIES  
FOR AEROASSISTED  
COPLANAR ORBITAL TRANSFER PROBLEM**

**D. S. Naidu, J. L. Hibey, and C. Charalambous  
Department of Electrical and Computer Engineering  
Old Dominion University  
Norfolk, VA**

**27th IEEE Conference on Decision and Control  
December 7–9, 1988  
Austin, Texas**

OUTLINE

- \* Aeroassist Technology
- \* Mission Description
- \* Problem Formulation
- \* Problem Solution
- \* Results
- \* Concluding Remarks



## SPACE TRANSPORTATION SYSTEMS

Low Cost Transportation is the Key to  
Exploration and Utilization of Space

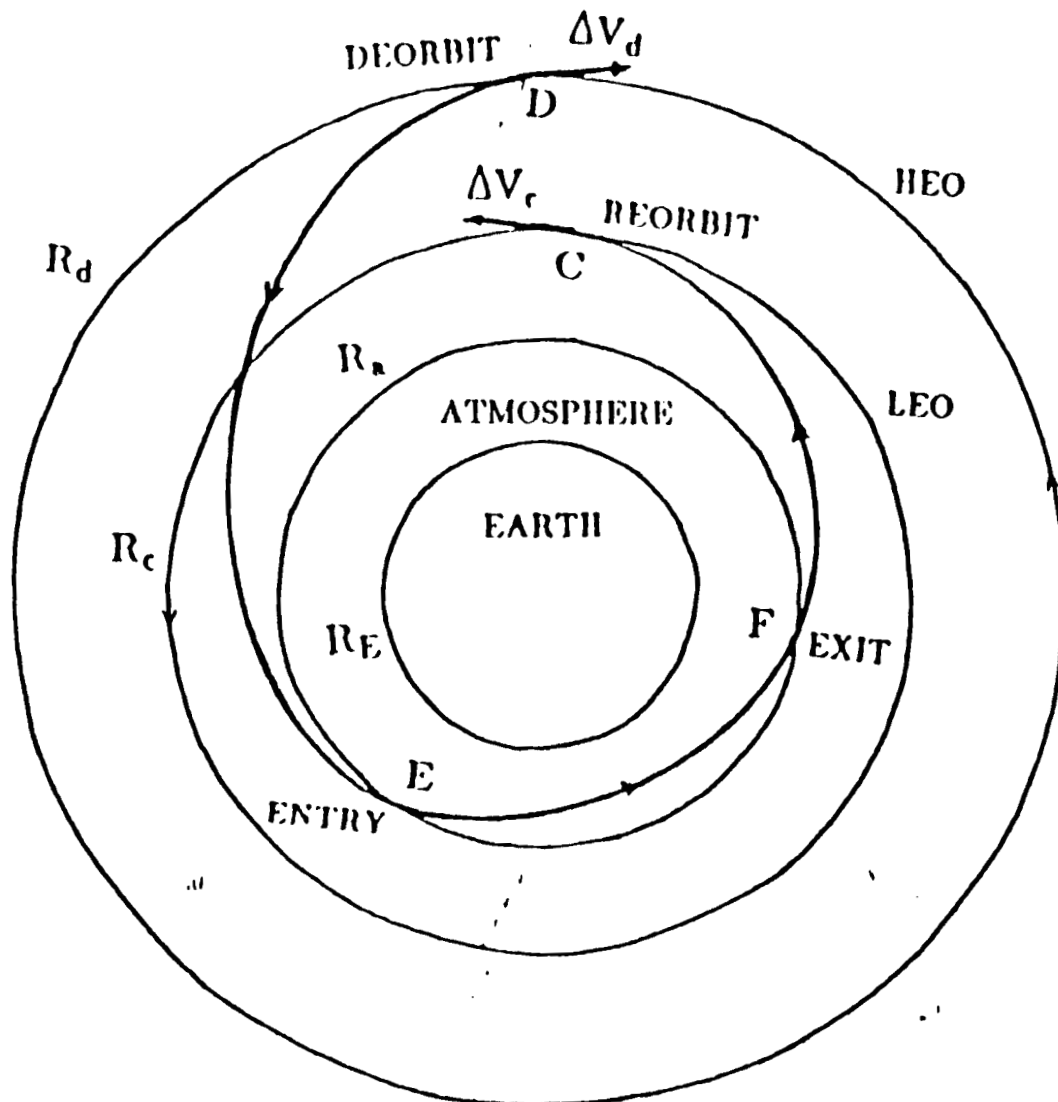
Orbital Transfer Vehicle (OTV) is an advanced upper stage concept for transportation of payloads from LEO such as Space Shuttle, Space Station to HEO such as GEO and other planetary excursions and return to a specified low earth parking orbit for reusability.

Aeroassist Technology is a technical capability for substantial reduction in propellant requirements by using the atmospheric (aeroassisted) maneuver on the return journey of the mission.

An orbital transfer vehicle utilizing the aeroassist technology becomes an Aeroassisted Orbital Transfer Vehicle (AOTV).

Advantages (1) High Performance, (2) Reusability

# MISSION DESCRIPTION



Aeroassisted coplanar orbital transfer

## PROBLEM FORMULATION

### Equations of Motion

$$dH/dt = V \sin \gamma$$

$$dV/dt = -AC_D V^2 \exp(-\beta H) - (\mu/R^2) \sin \gamma$$

$$d\gamma/dt = AC_L V \exp(-\beta H) - \{(V/R - \mu/(R^2 V))\} \cos \gamma$$

H : altitude; V : velocity;  $\gamma$  : flight path angle

$$A = S\rho_s/2m; \quad C_D = C_{D0} + KC_L^2; \quad \rho = \rho_s \exp(-\beta H)$$

## PROBLEM FORMULATION (Cont.)

### Performance Index

$$J = \Delta V = \Delta V_d + \Delta V_c$$

$$\Delta V_d = \sqrt{\mu/R_d} - (R_a/R_d)V_e \cos(-\gamma_e)$$

$$\Delta V_c = \sqrt{\mu/R_c} - (R_a/R_c)V_f \cos \gamma_f$$

$\Delta V_d$  : deorbit characteristic velocity at HEO

$\Delta V_c$  : circularizing characteristic velocity at LEO

## PROBLEM SOLUTION

The application of optimal control theory leads to a nonlinear, two-point, boundary value problem (TPBVP) with appropriate boundary conditions on state and costate variables.

For the entry and exit altitudes

$$H(t=0) = 120 \text{ km} = H(t=T)$$

For the HEO-to-entry elliptic transfer orbit

$$(2-v_e^2)a_d^2 - 2a_d + v_e^2\cos^2\gamma_e = 0$$

For the exit-to-LEO elliptic transfer orbit

$$(2-v_f^2)a_c^2 - 2a_c + v_f^2\cos^2\gamma_f = 0$$



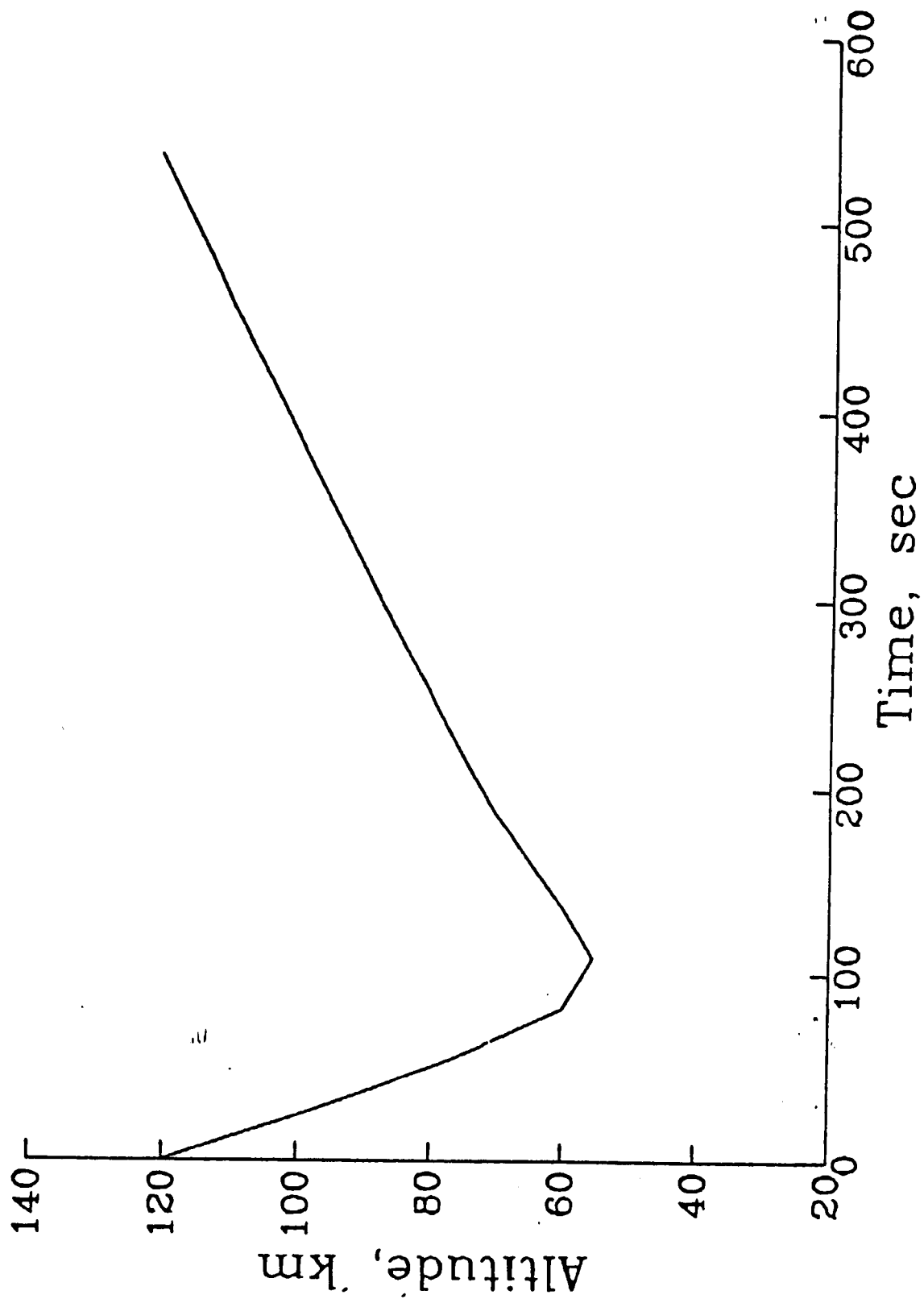
## PROBLEM SOLUTION (Cont.)

### Multiple Shooting Method

In the conventional (or simple shooting) method of solving TPBVP, we assume additional initial data and integrate forward so that the solution satisfies the given final conditions. The convergence of the solutions is highly sensitive to the assumed data.

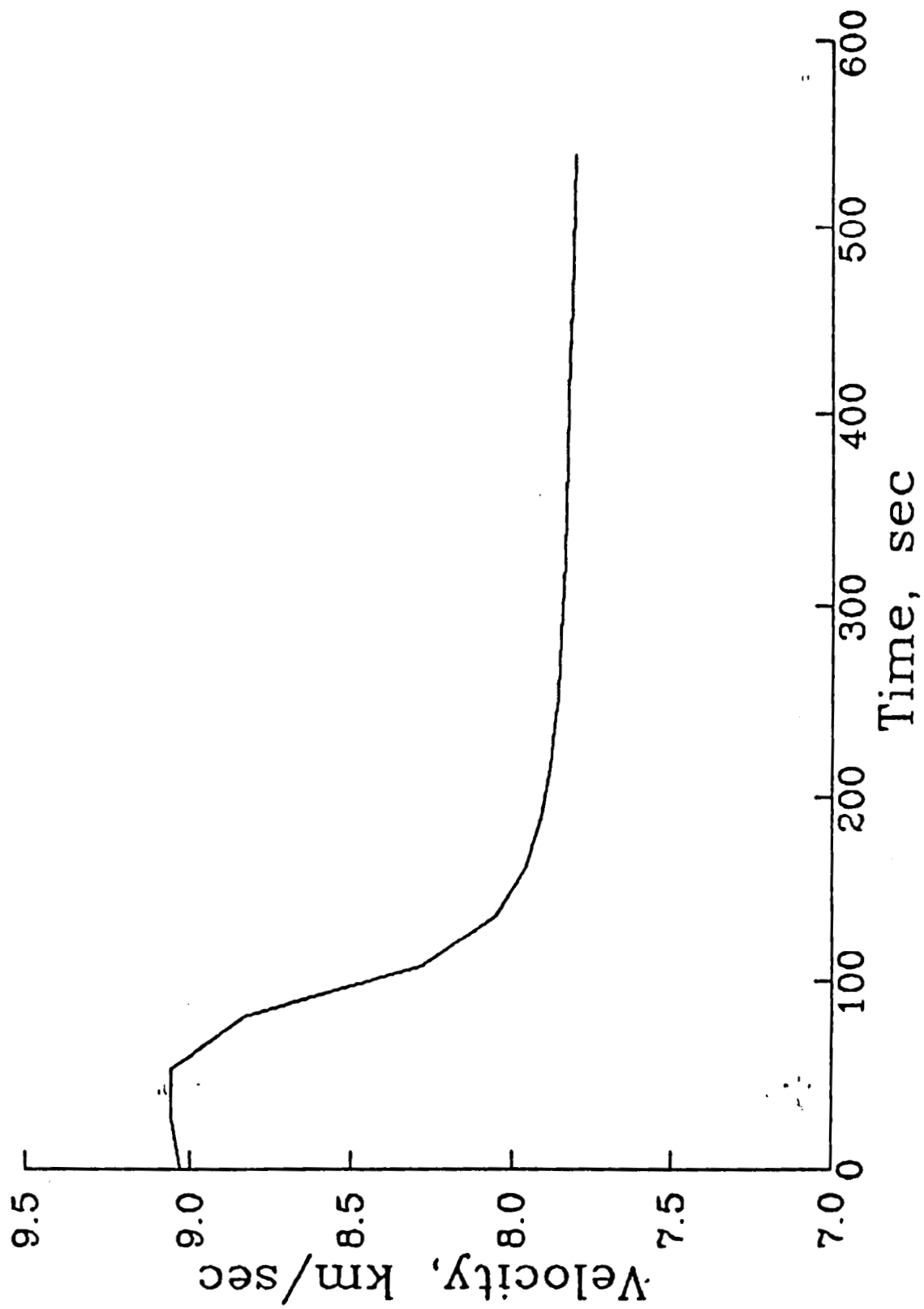
In the multiple shooting method, the whole interval is subdivided into smaller intervals with simultaneous application of simple shooting method over these subintervals. Here, the trajectory may be restarted at intermediate points using new guesses and finally reducing all the discontinuities at internal grid points to zero.

The corresponding OPTSOL code was developed by DFVLR at Oberpfaffenhofen, West Germany.

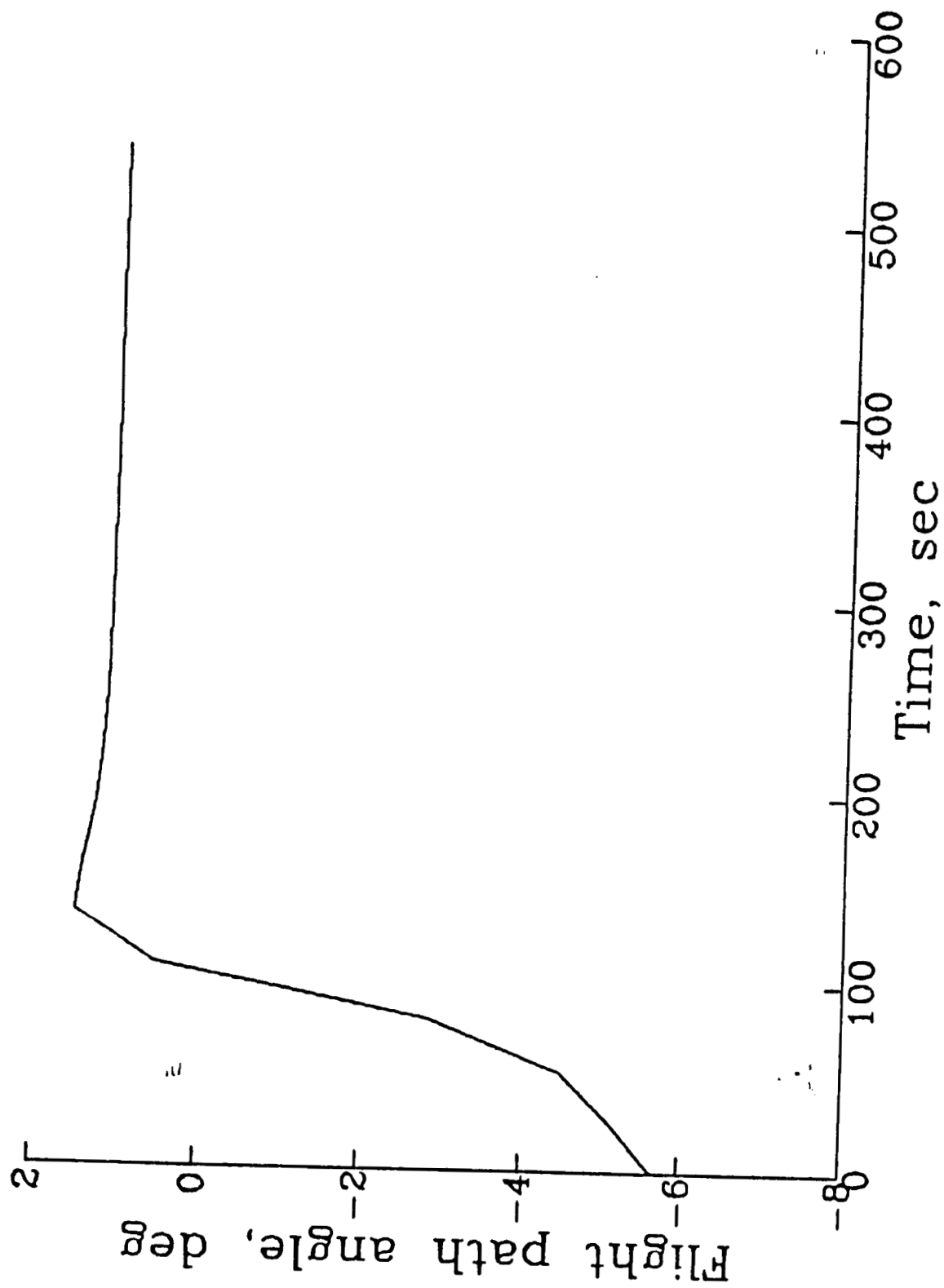


Time history of altitude

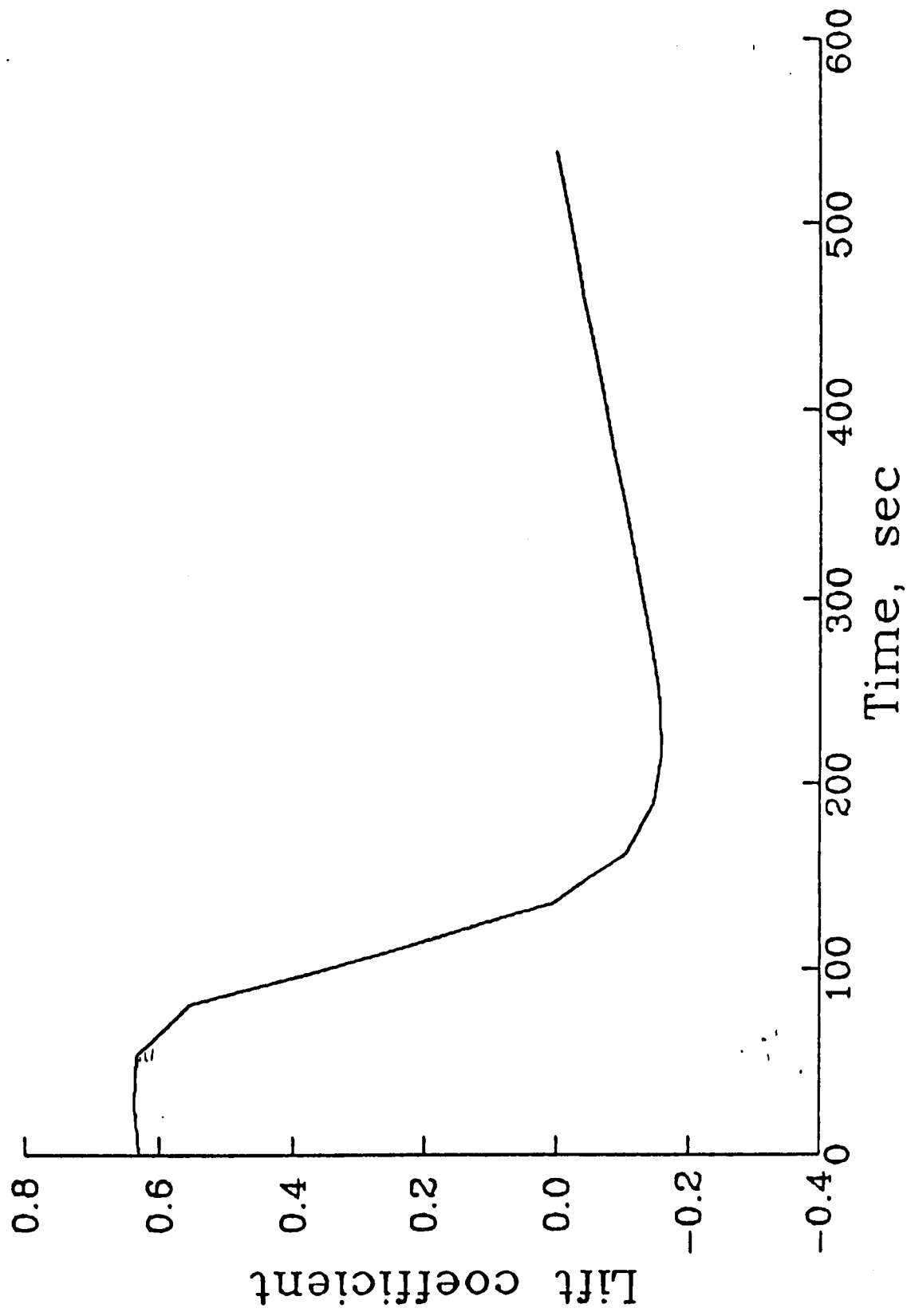
-11-



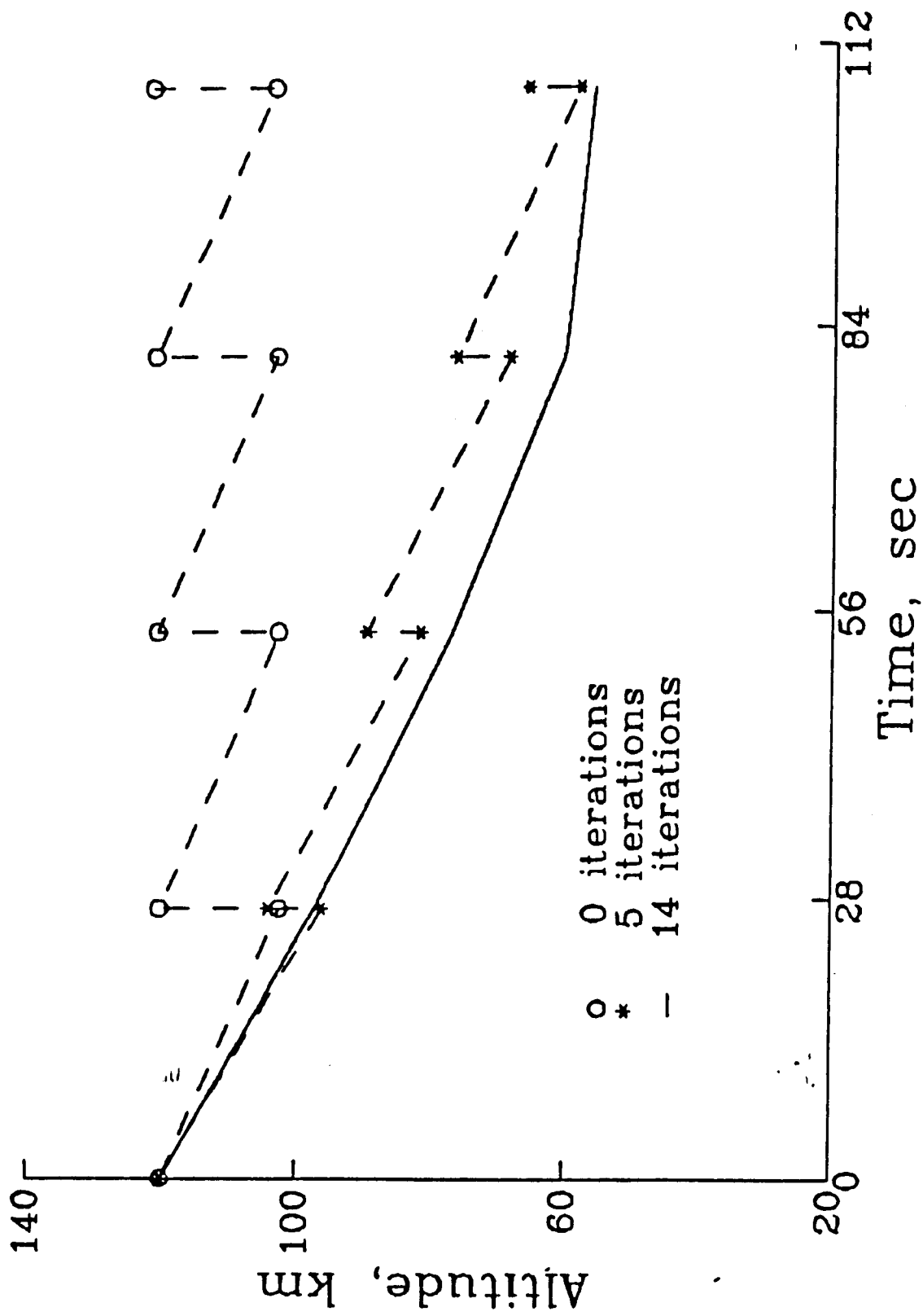
Time history of velocity



Time history of flight path angle



Time history of lift coefficient



Successive approximations for altitude

CONCLUDING REMARKS

1. Fuel optimal trajectories for noncoplanar orbital transfer problem have been obtained.
2. The strategy for the atmospheric portion of the minimum-fuel transfer is to fly at maximum L/D initially in order to recover from the downward plunge, and the vehicle skips out of the atmosphere with flight path angle near zero.
3. An efficient multiple shooting method has been used to solve the resulting TPBVP.
4. The multiple shooting method can be applied to solve the noncoplanar (plane change) orbital transfer problems.

FUEL-OPTIMAL TRAJECTORIES  
OF  
AEROASSISTED ORBITAL TRANSFER VEHICLES  
(summary)

Dr. D. S. Naidu  
Old Dominion University  
Norfolk, VA  
January 1989



**ABSTRACT:** The fuel-optimal control problem arising in orbital transfer vehicles employing aeroassist technology is addressed. The maneuver involves the transfer from high Earth orbit to low Earth orbit with plane change being performed during the atmospheric pass. A performance criterion is chosen to minimize the total fuel consumption for the transfer. The simulations are carried out using the industry standard POST program.

#### **NOMENCLATURE**

$g$  : gravitational acceleration  
 $g_s$  : gravitational acceleration at surface level  
 $H$  : altitude  
 $J$  : performance criterion  
 $m$  : vehicle mass  
 $R$  : distance from Earth center to vehicle center of gravity  
 $R_a$  : radius of the atmospheric boundary  
 $R_c$  : radius of the low Earth orbit  
 $R_d$  : radius of the high Earth orbit  
 $R_E$  : radius of Earth  
 $S$  : aerodynamic reference area  
 $L$  : aerodynamic reference length  
 $t$  : time  
 $V$  : velocity  
 $\gamma$  : flight path angle  
 $\sigma$  : bank angle  
 $\mu$  : gravitational constant of Earth  
 $\Delta V$  : characteristic velocity

#### **Subscripts**

$c$  : subscript for circularization or reorbit  
 $d$  : subscript for deorbit  
 $s$  : subscript for surface level

#### **1. INTRODUCTION**

In space transportation system, the concept of aeroassisted orbital transfer opens new mission opportunities, especially with regard to the initiation of a permanent space station [1]. The use of aeroassisted maneuvers to affect a transfer from high Earth orbit (HEO) to low Earth orbit (LEO) has

been recommended to provide high performance leverage to future space transportation systems. The space-based, orbit transfer vehicle (OTV) is planned as a system for transporting payloads between LEO and other locations in space. The OTV, on its return journey from HEO, dissipates orbital energy through atmospheric drag to slow down to LEO velocity. In a synergetic maneuver for aeroassisted, orbital transfer vehicles (AOTV's), the basic idea is to employ a hybrid combination of propulsive maneuvers in space and aerodynamic maneuvers in sensible atmosphere. Within the atmosphere, the trajectory control is achieved by means of lift and bank angle modulations. Hence, this type of flight with a combination of propulsive and nonpropulsive maneuvers, is also called synergetic maneuver or space flight[2-7].

An AOTV baseline mission is a round trip to GEO with a maximum return weight to LEO. In a typical mission [Fig.1], the AOTV with its payload is launched from Kennedy Space Center as a single Shuttle payload into a 296.5 km circular orbit inclined at 28.5 deg. The AOTV delivers its payload propulsively to GEO at 35810 km inclined at 0 deg. On its return journey, the vehicle dips into the atmosphere to achieve the necessary velocity depletion and inclination change and finally reaches the Space Station orbit at 556 km.

In this report, we obtain fuel-optimal trajectories for orbital transfer vehicles using aeroassist technology. The maneuver involves the transfer from HEO to LEO with a prescribed plane change and at the same time minimization of the fuel consumption. It is known that the change in velocity, also called the characteristic velocity, is a convenient parameter to measure the fuel consumption. For minimum-fuel maneuver, the objective is then to minimize the total characteristic velocity for deorbit, boost, and reorbit (or circularization). The simulations are carried out using the industry standard Program to Optimize Simulated Trajectories (POST) [8].

## 2. VEHICLE CONFIGURATIONS

In general, there are three types of AOTV configurations, depending on their lift/drag ratios [9].

(i) Low L/D configuration [Fig.2]: This, also called a lifting brake or an aerobrake, consists of a payload, propulsion, and miscellaneous subsystems that are packaged in a cylindrical structure. The aerobrake looking like a large umbrella of diameter 15.25m heat shield, is used for deceleration and inclination change by utilizing the drag and lift of the aerobrake at low angles of attack. The aerobrake is considered a low L/D concept with an experimental L/D of 0.25 at 15 deg angle of attack.

(ii) Moderate L/D configuration [Fig.3]: This has a cylindrical afterbody of 4.57m diameter with a raked-off nose to provide the necessary aerodynamic performance. The nose was designed for stagnation heating with an ablative shield. This configuration has a moderate L/D of 0.6 at 35 deg angle of attack.

(iii) High L/D configuration [Fig.4]: This vehicle has an estimated L/D of 2.18 at 11 deg angle of attack. For high L/D capability, the liquid oxygen is stored in two separate tanks to provide a tapered nose, and inflated chins are used to continue this tapering along the body. A large deployable flap is

needed to trim the vehicle at low angle of attack for maximum L/D performance.

### 3. MISSION DESCRIPTION

The mission comprises of deorbit, aeroassist (or atmospheric flight), boost and reorbit (or circularization) phases.

Initially, the spacecraft is in circular orbit of radius  $R_d$ , well outside the Earth's atmosphere, moving with a circular velocity  $V_d = \sqrt{\mu/R_d}$ . Deorbit is accomplished by means of an impulse  $\Delta V_d$ , to transfer the vehicle from a circular orbit to elliptic orbit with perigee low enough to intersect the dense part of the atmosphere. Since the elliptic velocity at D is less than the circular velocity at D, the impulse  $\Delta V_d$  is executed so as to oppose the circular velocity  $V_d$ . In other words, at point D, the velocity required to put the vehicle into elliptic orbit is less than the velocity required to maintain it in circular orbit. The deorbit impulse  $\Delta V_d$  causes the vehicle to enter the atmosphere at radius  $R_a$  with a velocity  $V_e$  and flight path angle  $\gamma_e$ . It is known that the optimal-energy loss maneuver from the circular orbit is simply the Hohmann transfer and the impulse is parallel and opposite to the instantaneous velocity vector.

Using the principle of conservation of energy and angular momentum at the deorbit point D, and the atmospheric entry point E, we get [10],

$$V_e^2/2 - \mu/R_a = (V_d - \Delta V_d)^2/2 - \mu/R_d \quad (1)$$

$$R_a V_e \cos(-\gamma_e) = R_d (V_d - \Delta V_d) \quad (2)$$

from which solving for  $\Delta V_d$ , we get

$$\Delta V_d = \sqrt{\mu/R_d} - \sqrt{2\mu(1/R_a - 1/R_d)/[(R_d/R_a)^2/\cos^2\gamma_e - 1]} \quad (3)$$

It is easily seen that the minimum value of the deorbit impulse  $\Delta V_{dm}$  obtained at  $\gamma_e = 0$ , corresponds to an ideal transfer with the space vehicle grazing the atmospheric boundary. To ensure proper atmospheric entry, deorbit impulse  $\Delta V_d$  must be higher than the minimum deorbit impulse  $\Delta V_{dm}$  which is given by

$$\Delta V_{dm} = \sqrt{\mu/R_d} - \sqrt{2\mu(1/R_a - 1/R_d)/[(R_d/R_a)^2 - 1]} \quad (4)$$

During the aeroassist (or atmospheric flight), the vehicle needs to be

controlled by lift and/or bank angle to achieve the necessary velocity reduction (due to atmospheric drag) and the plane change. Because of the loss of energy during a turn, a second impulse is required to boost the vehicle back to orbital altitude.

The vehicle exits the atmosphere at point F, with a velocity  $V_f$  and flight path angle  $\gamma_f$ . The additional impulse  $\Delta V_b$ , required at the exit point F for boosting into an elliptic orbit with apogee radius  $R_c$  and the reorbit (or circularization) impulse  $\Delta V_c$  required to insert the vehicle into a circular orbit, are obtained by using the principle of conservation of energy and angular momentum at the exit point F, and the reorbit or circularization point C. Thus, we have,

$$(V_f + \Delta V_b)^2/2 - \mu/R_a = (V_c - \Delta V_c)^2/2 - \mu/R_c \quad (5)$$

$$(V_f + \Delta V_b)R_a \cos \gamma_f = R_c (V_c - \Delta V_c) \quad (6)$$

Solving for  $\Delta V_b$  and  $\Delta V_c$  from the above equations (5) and (6),

$$\Delta V_b = \sqrt{2\mu(1/R_a - 1/R_c) / [1 - (R_a/R_c)^2 \cos^2 \gamma_f]} - V_f \quad (7)$$

$$\Delta V_c = \sqrt{\mu/R_c} - \sqrt{2\mu(1/R_a - 1/R_c) / [(R_c/R_a)^2 / \cos^2 \gamma_f - 1]} \quad (8)$$

#### 4. TRAJECTORY SIMULATION

It is known that the change in speed,  $\Delta V$ , also called the characteristic velocity, is a convenient parameter to measure the fuel consumption. For minimum-fuel maneuver, the objective is then to minimize the total characteristic velocity. A convenient performance index is the sum of the characteristic velocities for deorbit, boost, and reorbit. Thus,

$$J = \Delta V_d + \Delta V_b + \Delta V_c \quad (9)$$

Where,  $\Delta V_d$ ,  $\Delta V_b$ , and  $\Delta V_c$  are the deorbit, boost, and reorbit characteristic velocities respectively, and are related as

$$\Delta V_d = \sqrt{\mu/R_d} - (R_a/R_d)V_e \cos(-\gamma_e) \quad (10)$$

$$\Delta V_c = \sqrt{\mu/R_c} - (R_a/R_c)(V_f + \Delta V_b) \cos \gamma_f \quad (11)$$

Let us note that for a given circular orbit, the impulses  $\Delta V_b$  and  $\Delta V_c$  are completely determined by the variables  $V_f$  and  $\gamma_f$  at the exit conditions of the atmospheric portion of the trajectory. The velocity  $V_e$  and the flight path angle  $\gamma_e$  at the entry point are dependent only on the magnitude of the deorbit impulse  $\Delta V_d$ . Therefore, the optimal trajectory problem needs to consider the segment of the trajectory within the atmosphere.

Trajectories for the AOTV are calculated using the three-dimensional version of the Program to Optimize Simulated Trajectories (POST) [13]. A 1976 US standard atmosphere is used. The results are given for the high L/D configuration only. Similar results are obtained for the other low L/D and moderate L/D configurations and will be reported separately.

A propulsive maneuver with impulsive burn having a characteristic velocity ( $\Delta V_b$ ) of 1491.25 m/sec and a specific impulse of 456 sec targets the AOTV with a transfer orbit perigee of that lies within the Earth's atmosphere. Some of the plane change to reacquire the Shuttle inclination is accomplished during this maneuver and the remaining being obtained from aeromaneuvering capability of the AOTV. Upon reaching the atmosphere interface at 120km, the AOTV flies the aerodynamic portion of its trajectory at constant angle of attack but with variable bank angle, rolling the lift vector about the velocity vector. Rotating the lift vector modulates the drag via altitude control but also turns the vehicle through the remaining inclination change. The aeroassist phase of the mission ends as the AOTV exits through the atmospheric boundary at 120km. Sufficient energy is dissipated during the aerobraking for the orbit apogee to be reduced to 556km, the assumed orbit for subsequent Space Station rendezvous.

A typical set of numerical values used for simulation purposes is given below [8].

weight of the vehicle excluding the payload = 112,625 N  
aerodynamic reference area of the vehicle = 30.8 sq.m  
aerodynamic reference length of the vehicle = 15.67m

Using the above mentioned data, simulations are carried out for obtaining the nominal trajectories using POST. The nominal solution has the following entry and exit status.

Entry status:  $H_e = 120$  km;  $V_e = 10306$  m/sec  
 $\gamma_e = -5.1541$  degrees;  $i_e = 0$  deg  
Exit status:  $H_f = 120$  km;  $V_f = 8062.5$  m/sec  
 $\gamma_f = 1.9484$  deg;  $i_f = 23.039$  deg  
total flight time = 579.2 sec

Time histories of altitude  $H$ , velocity  $V$ , and flight path angle  $\gamma$ , for

total flight time of 579 seconds, are shown in Figures 5-7 respectively. The variation of bank angle and orbit inclination are depicted in Figures 8 and 9. Those for the heating rate, and dynamic pressure are shown in Figures 10 and 11.

Figure 5 shows the time history of altitude. The spacecraft enters and exits the atmosphere at an altitude of 120 km. The minimum altitude reached is 55.47 km. The velocity versus time is shown in Figure 6. The vehicle enters the atmosphere with a velocity of 10306 m/sec and leaves the atmosphere with a speed of 8062.5 m/sec, thus giving a velocity reduction of 1243.5 m/sec. The profile of flight path angle with time is shown in Figure 7. The spacecraft enters the atmosphere with an inclination of -5.1541 degrees and exits with 1.9484 degrees. Figure 8 shows the variation of bank angle during the atmospheric flight. Initially the vehicle enters the atmosphere with a bank angle of -60.76 degrees to pull the vehicle into the atmosphere and decreases further to -105 deg and approaches zero degrees at the exit of the atmosphere. Fig. 9 shows the variation of orbit inclination. At the entry the inclination is assumed to be 0 degrees and at the exit the vehicle acquires an inclination of 23.04 degrees and any further inclination required may be obtained propulsively.

## 5. CONCLUDING REMARKS

In this report, we have addressed the minimization of fuel consumption during the atmospheric portion of an aeroassisted, noncoplanar, orbital transfer vehicles. The simulations are carried out for a high L/D configuration using the industry standard Program to Optimize Simulated Trajectories (POST) [13]. The results for other moderate L/D and low L/D configurations are being investigated and will be reported separately.

## ACKNOWLEDGEMENTS

This research work was supported by the grant NAG1-736 under the technical monitorship of Dr. Douglas B. Price, Acting Head, Spacecraft Control Branch, NASA Langley Research Center, Hampton.

## 6 References

1. Walberg, G. D., "A survey of aeroassisted orbital transfer", J. Spacecraft, 22, 3-18, Jan.-Feb., 1985.
2. Vinh, N.-X., Optimal Trajectories in Atmospheric Flight, Elsevier Scientific Publishing Co., Amsterdam, 1981.
3. Dickmann, E. D., The effect of finite thrust and heating constraints on the synergetic plane change maneuver for space-shuttle orbiter-class vehicle, NASA TN D-7211, Oct. 1973.
4. Hull, D. G., Glitner, J. M., Speyer, J. L., and Maper, J., "Minimum energy loss guidance for aeroassisted orbital plane change", J. Guidance, Control, and Dynamics, 8, 487-493, July-Aug., 1985.

5. Vinh, N. X., and Hanson, J. M., "Optimal aeroassisted return from high Earth orbit with plane change", Acta Astronautica, 12, 11-25, 1985.
6. Miele, A., Baspur, V. K., and Lee, W. Y., "Optimal trajectories for aeroassisted noncoplanar orbital transfer", Acta Astronautica, 15, 399-412, June-July, 1987.
7. Mishne, D., and Speyer, J. L., "Optimal control of aeroassisted plane change maneuver using feedback expansions", Proc. AIAA Flight Mechanics Conf., Williamsburg, Aug., 1986.
8. Brauer, G. L., Cornick, D. E., and Stevenson, R., "Capabilities and Applications of the Program to Optimize Simulated Trajectories (POST)," NASA CR-2770, Feb. 1977.
9. Talay, T. A., White, N. H., and Naftel, J. C., "Impact of atmospheric uncertainties and viscous interaction effects on the performance of aeroassisted orbital transfer vehicles," AIAA 22nd Aerospace Science Meeting, Reno, NV, Jan. 1984.
10. Kaplan, M. H., Modern Spacecraft Dynamics and Control, John Wiley & Sons, New York, 1976.

\*\*\*\*\*

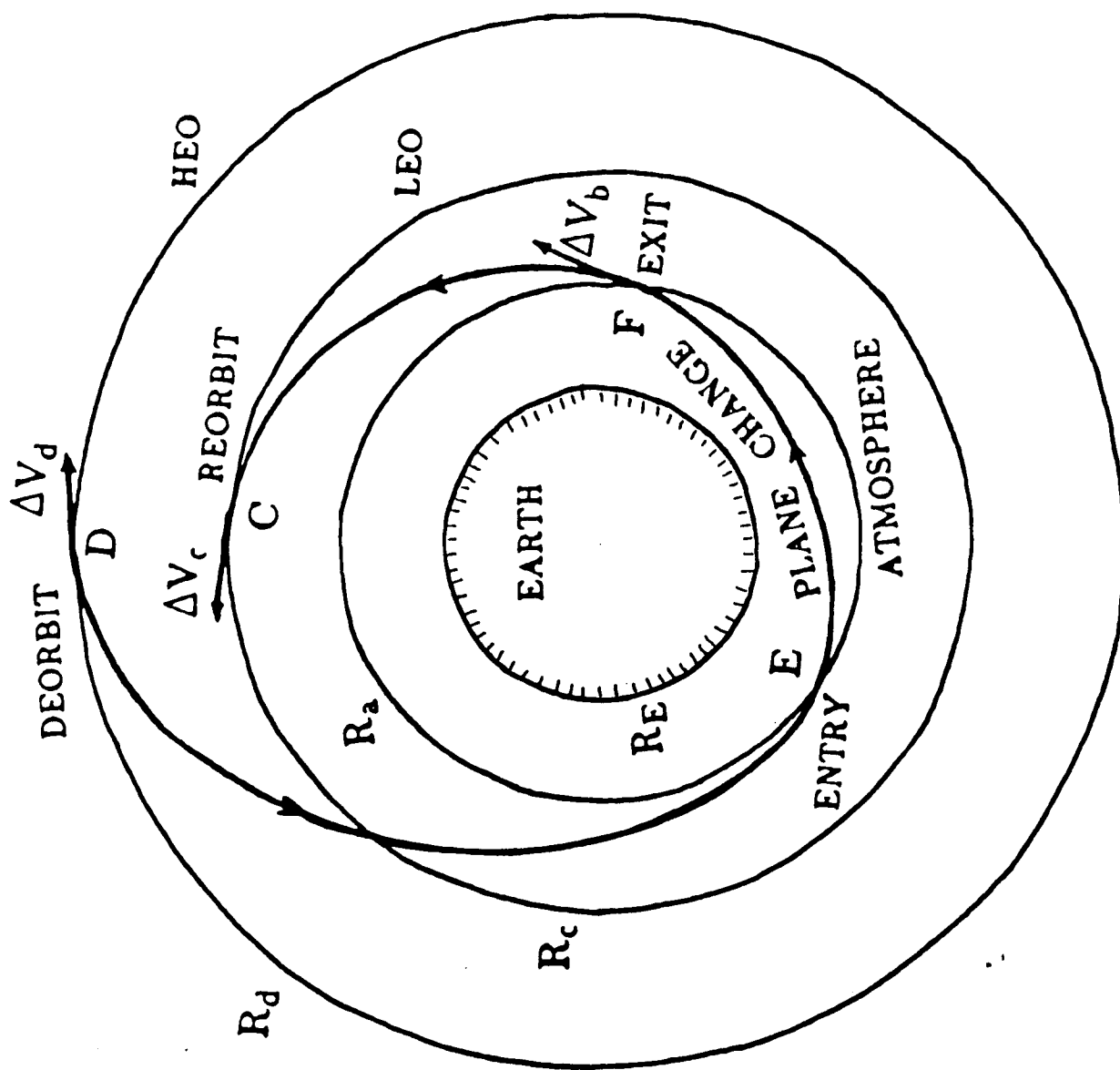


Fig.1 Aeroassisted orbital transfer with plane change



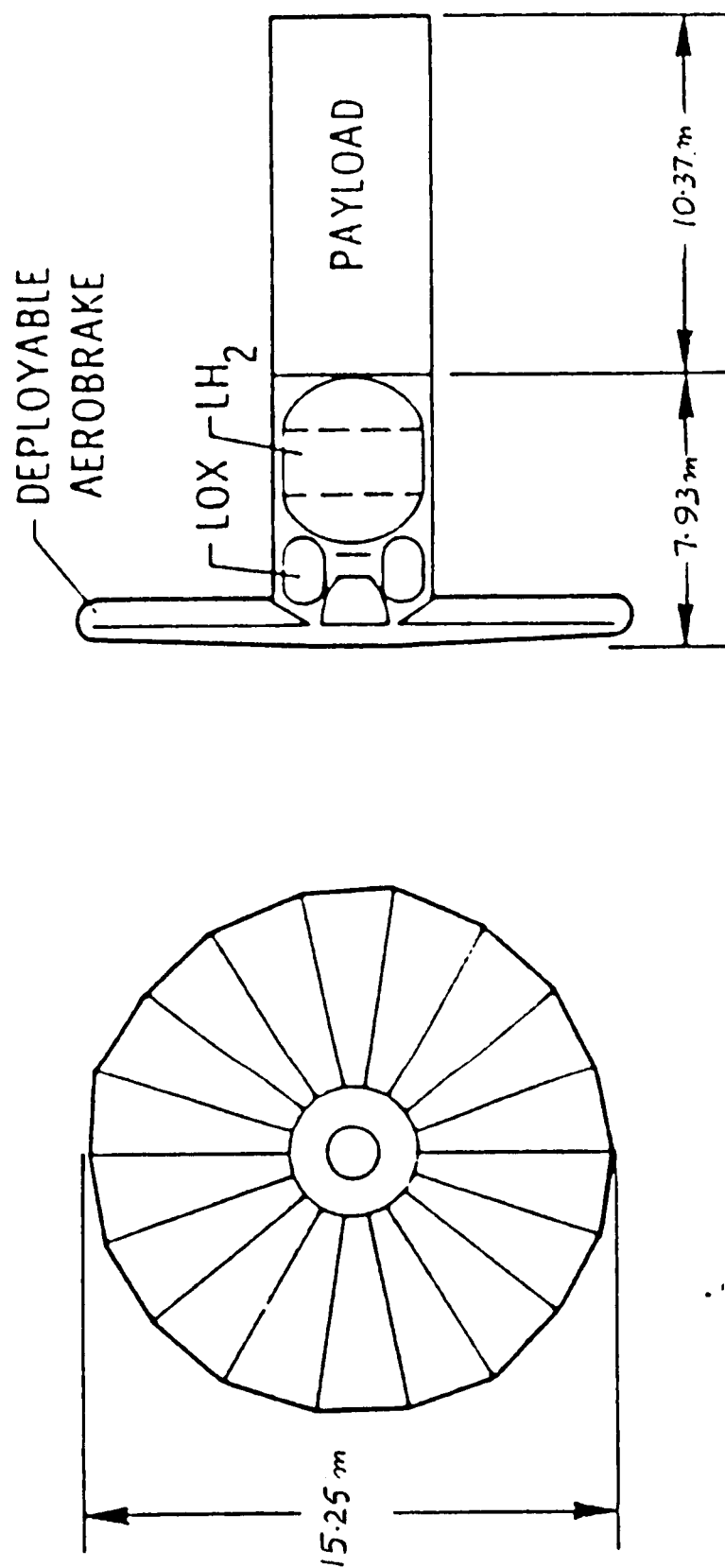


Fig.2 Low L/D configuration

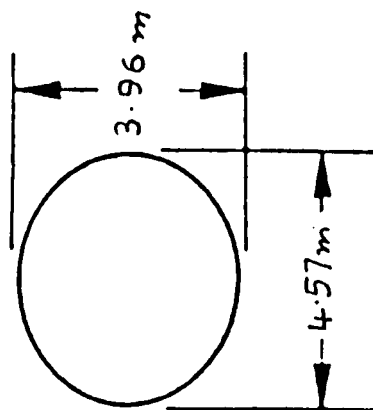
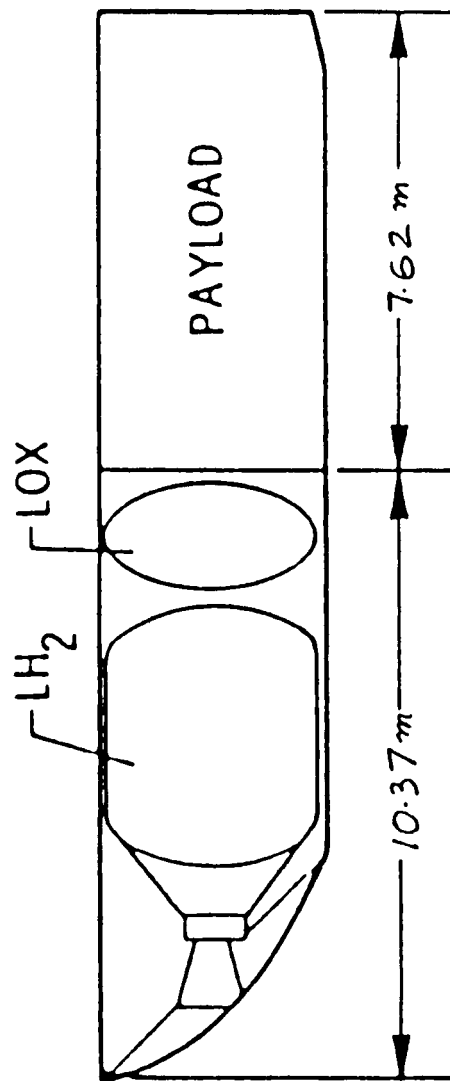
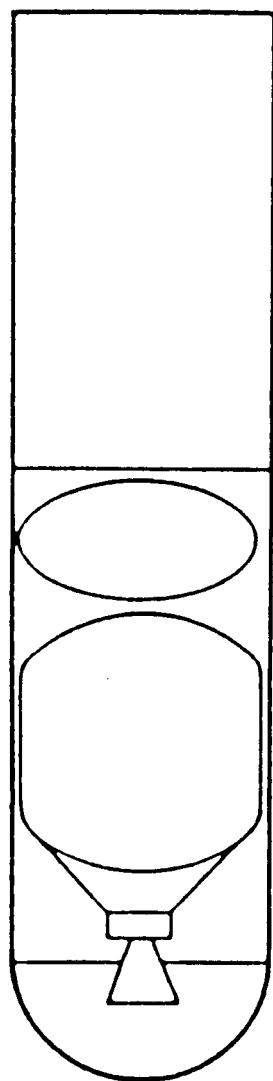


Fig.3 Moderate L/D configuration

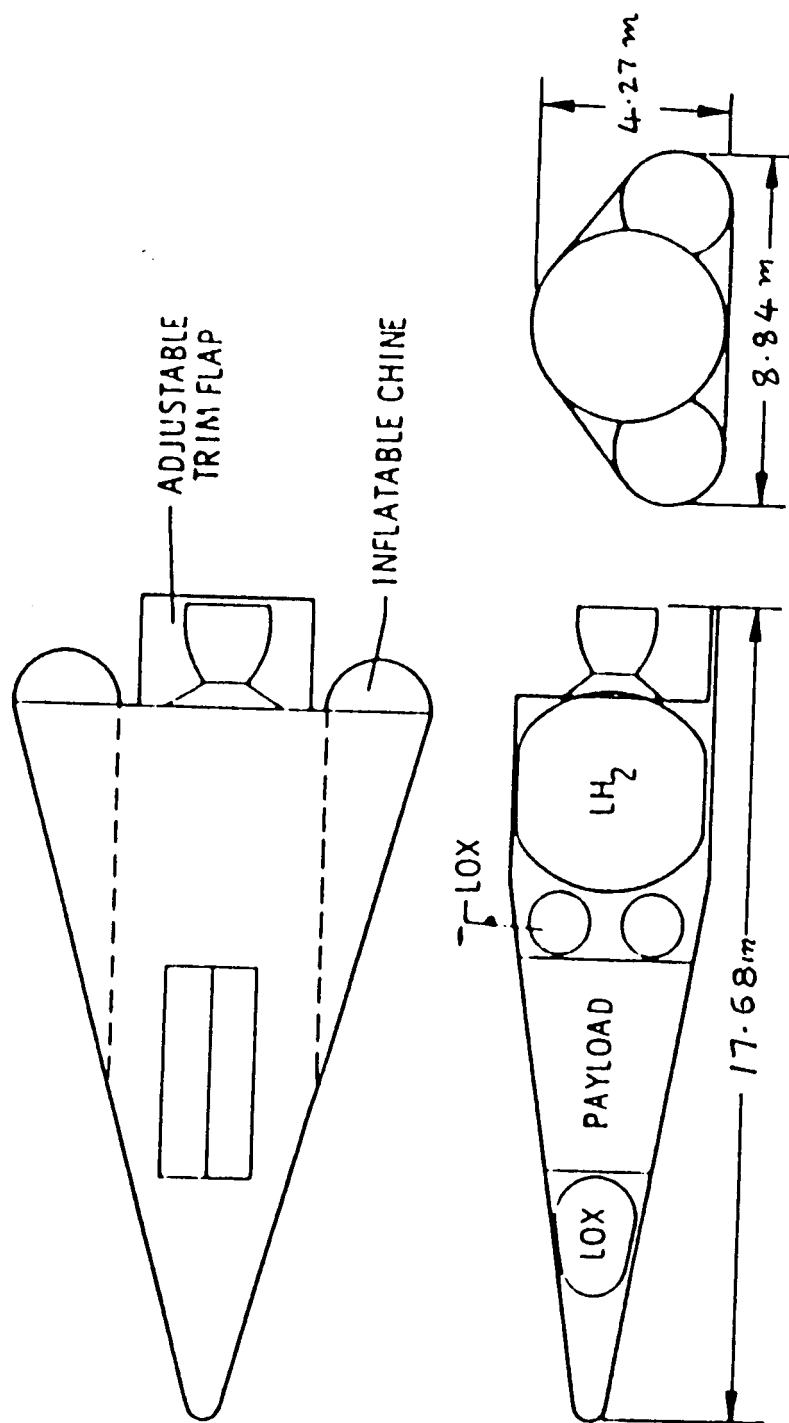


Fig.4 High L/D configuration

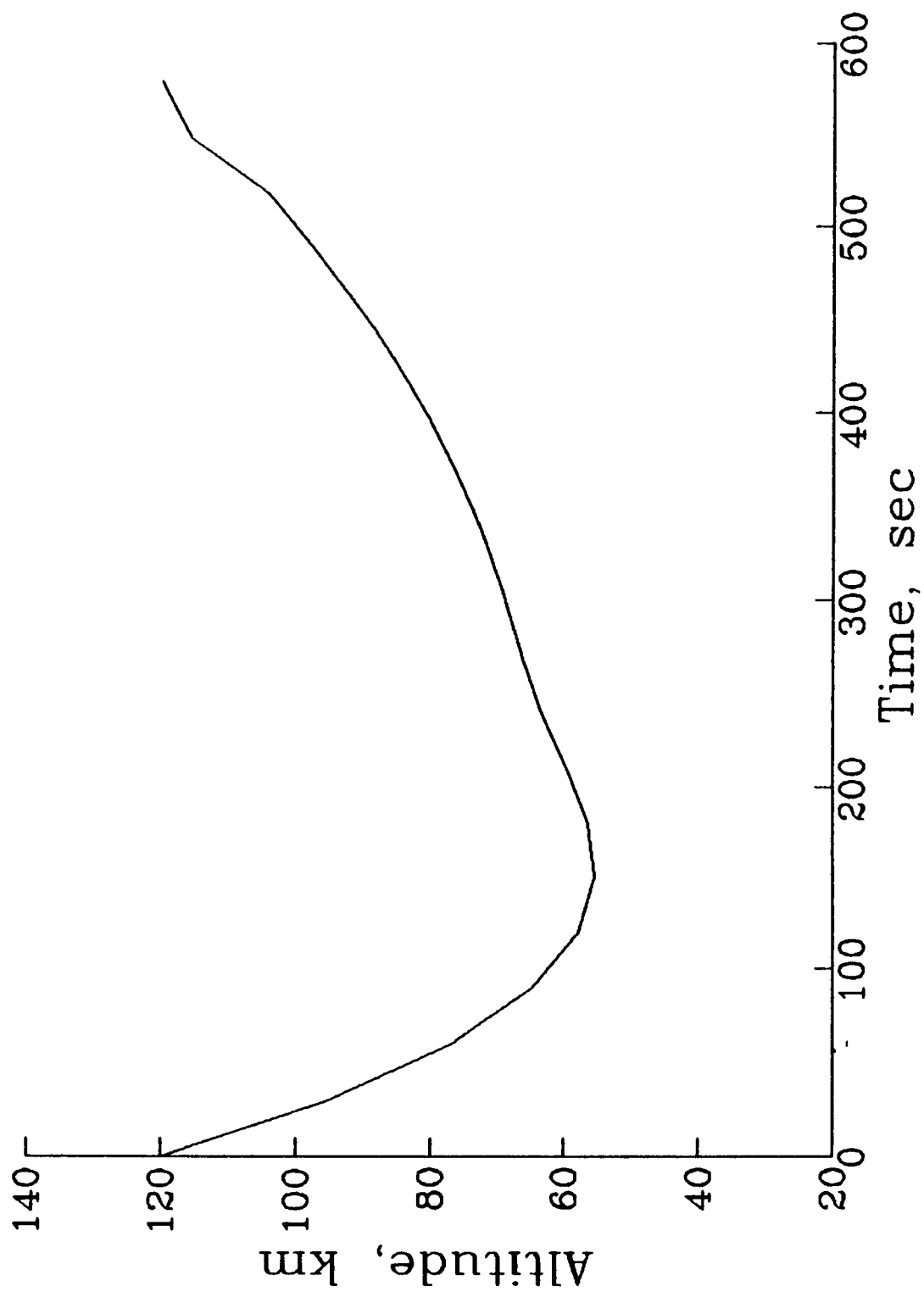


Fig.5 Time history of altitude

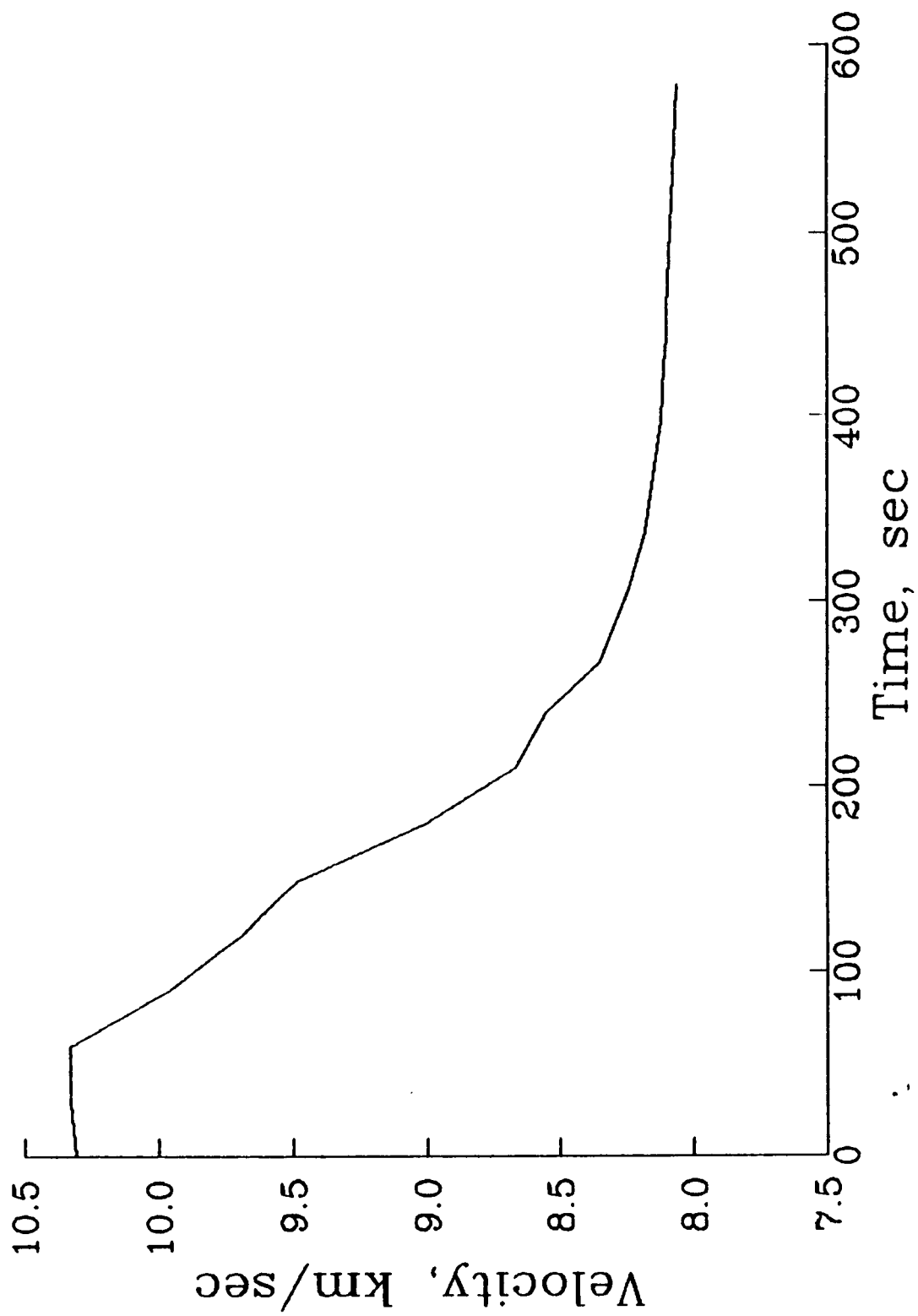


Fig.6 Time history of velocity

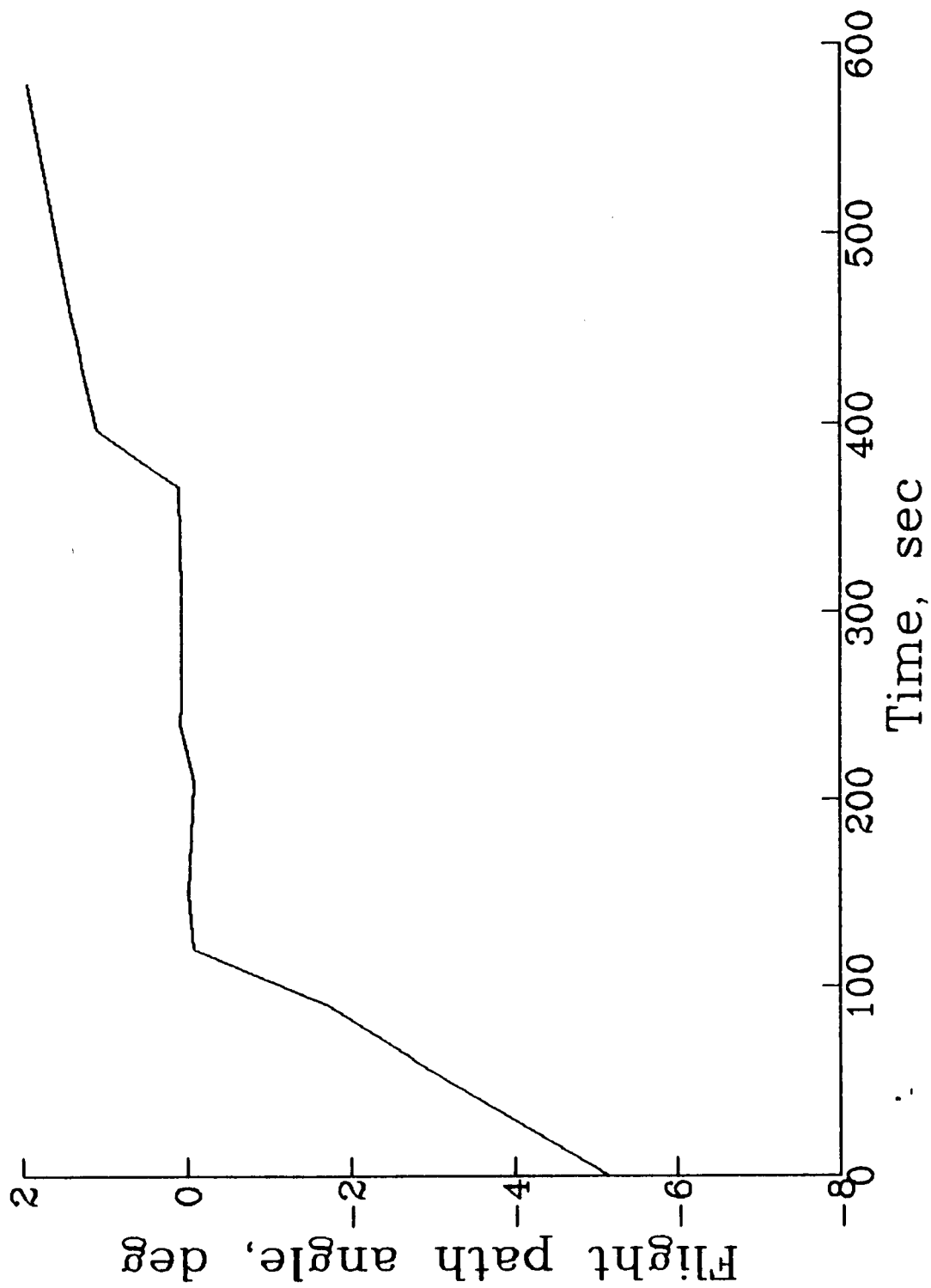


Fig.7 Time history of flight path angle

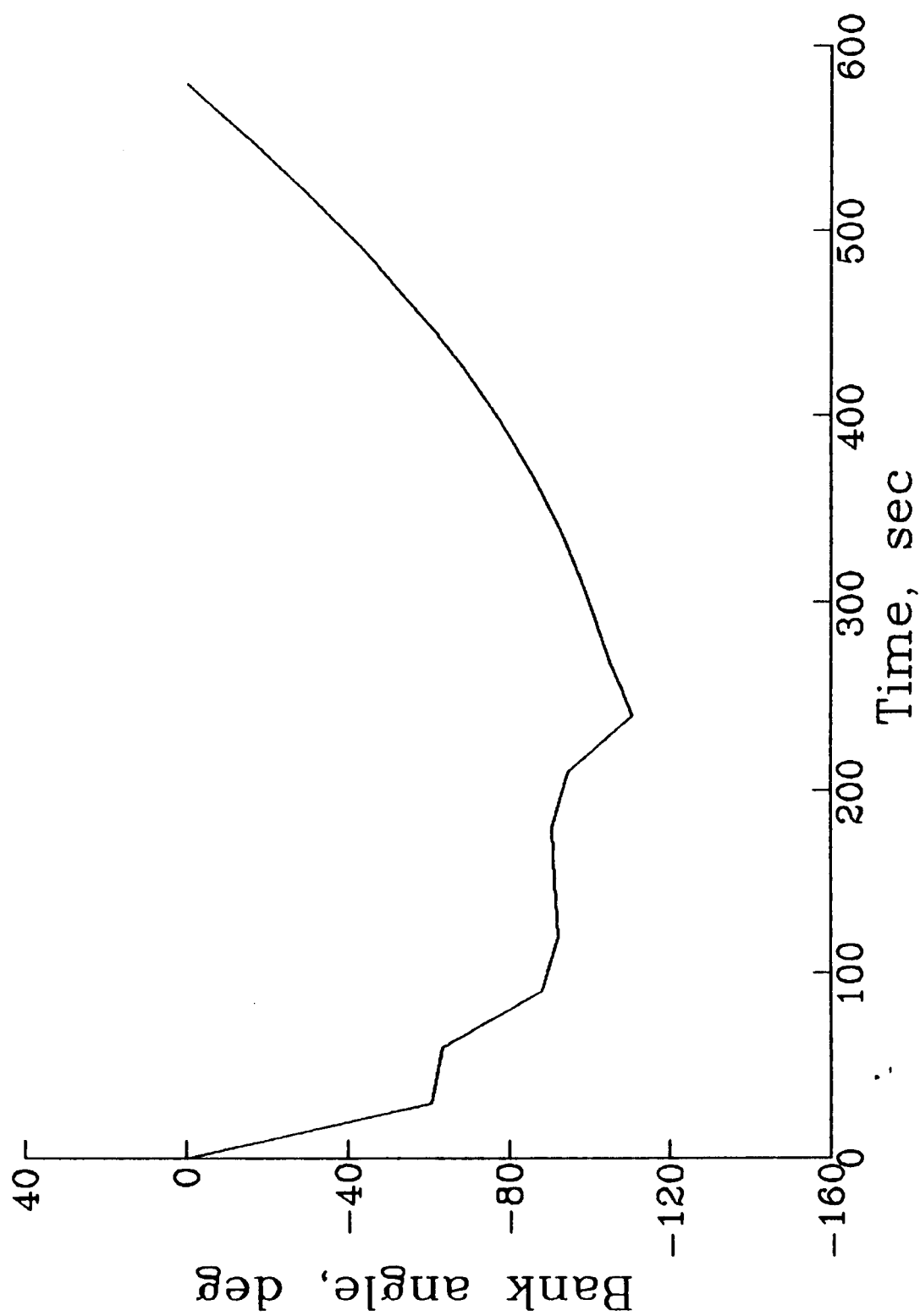


Fig.8 Time history of bank angle

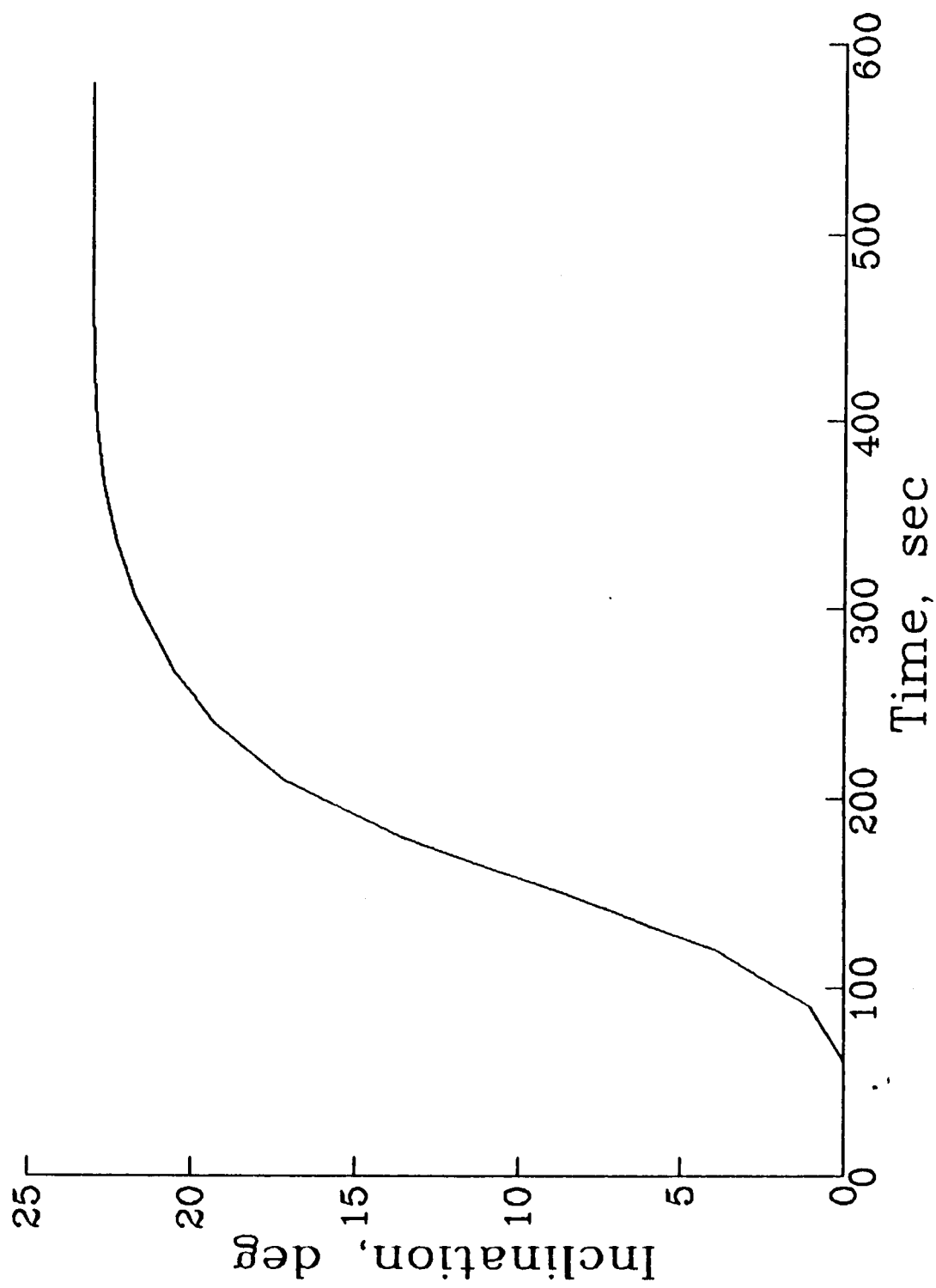


Fig.9 Time history of inclination



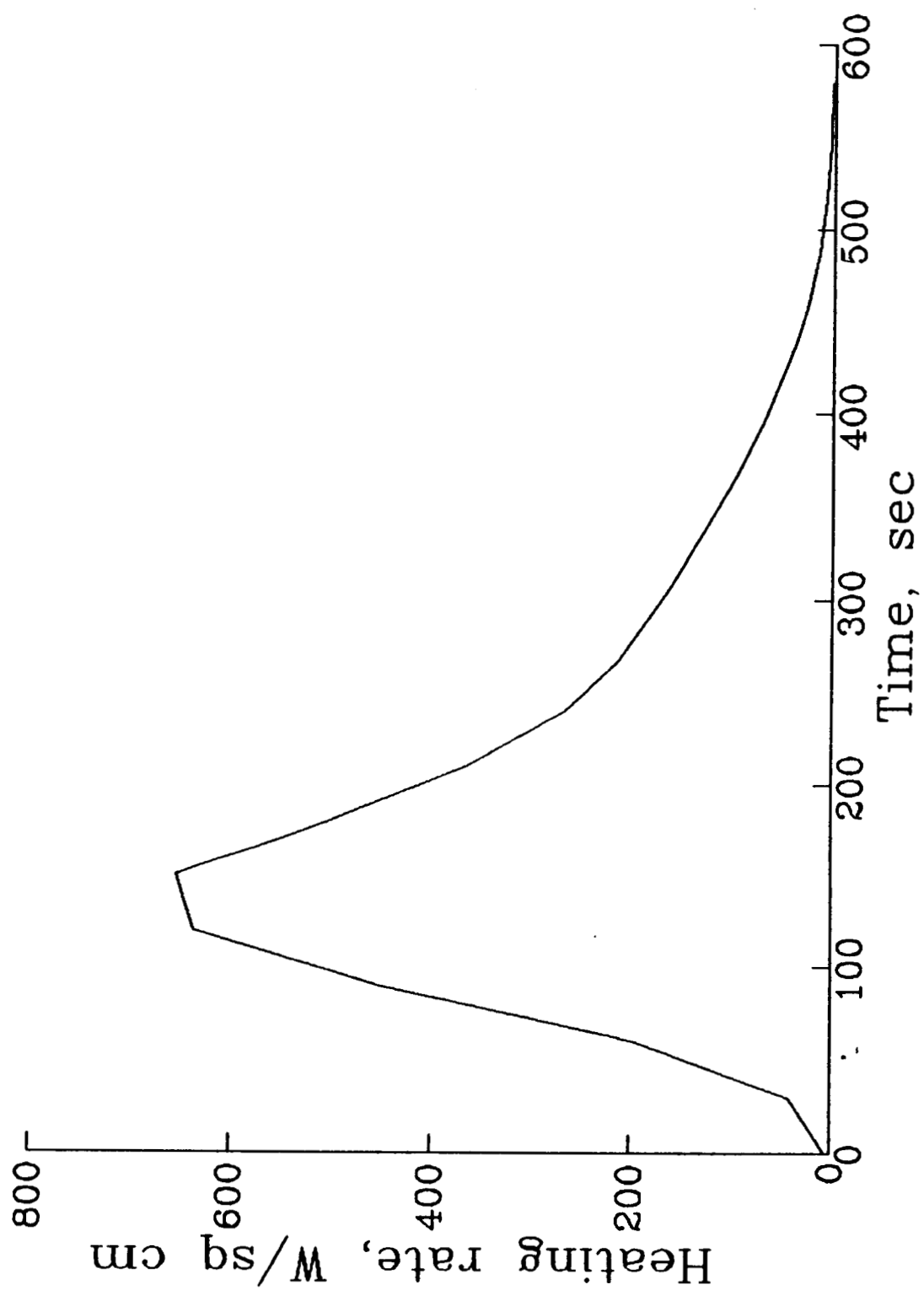


Fig.10 Time history of heating rate